IEEE Access
Multidisciplinary ⋮ Rapid Review ⋮ Open Access Journal

Received 25 January 2023, accepted 16 February 2023, date of publication 22 February 2023, date of current version 1 March 2023.

Digital Object Identifier 10.1109/ACCESS.2023.3247977

RESEARCH ARTICLE

Distributed Energy Resources Electric Profile Identification in Low Voltage Networks Using Supervised Machine Learning Techniques

ANDRES F. MORENO JARAMILLO[1,2], (Member, IEEE), JAVIER LOPEZ-LORENTE[3], (Member, IEEE), DAVID M. LAVERTY[1], (Senior Member, IEEE), PAUL V. BROGAN[4], SANTIAGO H. HOYOS VELASQUEZ[5], (Member, IEEE), JESUS MARTINEZ-DEL-RINCÓN[1], AND AOIFE M. FOLEY[6,7,8], (Senior Member, IEEE)

[1]School of Electronics, Electrical Engineering and Computer Science, Queen's University Belfast, BT9 6SB Belfast, U.K.
[2]Future Networks, NIE Networks, BT3 9JQ Belfast, U.K.
[3]PV Technology Laboratory, Department of Electrical and Computer Engineering, FOSS Research Centre for Sustainable Energy, University of Cyprus, 1678 Nicosia, Cyprus
[4]Data Applications, Phasora Ltd., BT12 7DG Belfast, U.K.
[5]EnergEIA Research Cluster, EIA University, Envigado, Antioquia 055413, Colombia
[6]School of Mechanical and Aerospace Engineering, Queen's University Belfast, BT7 1NN Belfast, U.K.
[7]Mechanical, Aerospace and Civil Engineering, School of Engineering, The University of Manchester, M13 9PL Manchester, U.K.
[8]Electrical and Electronic Engineering, School of Engineering, The University of Manchester, M13 9PL Manchester, U.K.

Corresponding author: Andres F. Moreno Jaramillo (amorenojaramillo01@qub.ac.uk)

This work is part of the Collaborative REsearch of Decentralization, ElectrificatioN, Communications and Economics (CREDENCE) project, which is funded by a US-Ireland, Department for the Economy (DfE) Research, Science Foundation Ireland (SFI), National Science Foundation (NSF) and Development Partnership Program (Centre to Centre) award (grant number USI 110). Dr David Laverty has also received support from the Engineering and Physical Sciences Research Council (EPSRC) through 'i-Give' (EP/L001063/1) and the Converged Approach towards Resilient Industrial control systems and Cyber Assurance (CAPRICA) (EP/M002837/1) projects. The work of J. Lopez-Lorente was co-funded by the European Regional Development Fund and the Republic of Cyprus through the Cyprus Research and Innovation Foundation under the ''Modernising the distribution grid for enabling high penetration of photovoltaic electricity through advanced data analytic operational observability and management'' (ELECTRA) project (INTEGRATED/0918/0071).

ABSTRACT Increasing integration of distributed energy resources (DER) in the electrical network has led distribution network operators to unprecedented challenges. This issue is compounded by the lack of monitoring infrastructure on the low voltage (LV) side of distribution networks at residential and utility sides. Non-intrusive load monitoring (NILM) methods provide an opportunity to add value to conventional electric measurements and to increase the observability of LV networks for the implementation of active management network techniques and intelligent control of DER. This work proposes a novel implementation of NILM methods for the identification of DER electrical signatures from aggregated measurements taken at the LV side of a distribution transformer. The implementation evaluates three machine learning algorithms such as k Nearest Neighbours (kNN), random forest and a multilayer perceptron under 100 scenarios of DER integration. A year of minutely reported values of electric current, voltage, active power, and reactive power are used to train and test the proposed model. The F_1 scores achieved of 73% and 93% for Electrical Vehicles (EV) and rooftop photovoltaic (PV) respectively and processing times below 314 μs on an Intel Core i7-8700 machine. These results confirm the relevance of the NILM method based on low frequency electric measurements from the real-time identification of DER.

INDEX TERMS Distributed energy resources (DER), non-intrusive load monitoring (NILM), low voltage networks distribution networks (LVN), random forest, supervised machine learning.

I. INTRODUCTION

The power generation industry is accountable for 38% of the global carbon dioxide emissions and it is one of the

The associate editor coordinating the review of this manuscript and approving it for publication was Wentao Fan.

main sectors targeted on national and international policies towards net carbon emission targets [1]. The electrification of transport and heating sectors have brought unprecedented changes modifying the dynamics of the electrical network. Particularly, electrical characteristics of low voltage (LV) distribution networks are increasingly varying due to a rapid integration of distributed energy resources (DER), forcing distribution network operators (DNO) to manage old electrical infrastructure near and beyond their operational limits [2].

The decarbonization of industrial sectors, significant technological advances, improved efficiency, and increased affordability represent some of the main drivers for customers (and producer-consumers, also called 'prosumers') to acquire DER, mainly connected to LV distribution networks [3]. Technical constraints from DER are compounded with a low (or null) observability of LV electrical networks, which leads DNO to face unprecedented operational challenges [4].

Distribution network operators have been working towards more observable LV distribution networks to implement advanced control measures based on higher flexibility and active management network schemes [5]. Consequently, the availability of electrical records such as electric current, voltage and power of LV distribution networks enables the implementation of more advanced monitoring techniques such as non-intrusive load monitoring (NILM) methods. Improved monitoring increases the accuracy of electrical maps, including DER locations and enables the implementation of advanced demand side management (DSM) techniques and flexibility schemes [6].

In this work, a supervised NILM method is proposed to identify DER electric patterns at the LV side of a distribution transformer. The proposed NILM method is built and evaluated using the IEEE European LV Voltage test feeder [7] with 1-minute resolution data of electric current, voltage, active and reactive power model using EPRI's Open Distribution System Simulator (OpenDSS) [8]. A total of 100 EV and PV integration scenarios are evaluated to scrutinise the performance of various classification methods based on kNN [9], Random Forest (RF) [10], and multilayer perceptron (MLP) [11] machine learning algorithms.

The main motivation of this research consists of covering a research gap found on the implementation of NILM methods for the identification of several DER from aggregated measurements at low voltage distribution levels. This enhances the electrical network maps, which positively impacts the electrical network stakeholders in technical, economic, social, and environmental aspects. Therefore, informing DNO for more efficient planning and operation of LV networks with optimised control systems. This allows the optimal integration of DER towards the decarbonisation of the electrical sector and the electrification of the transport and heating sectors. In addition, this paper presents the first evaluation of NILM approaches for individual and combined aggregated measurements at phase level on the LV side of distribution transformers.

This work is based on preliminary research presented in [12] where a NILM method based on kNN was evaluated. The classification method served as base case to observe the performance of the proposed model to identify EV and PV systems. In total, 50 scenarios were used to assess the performance of the NILM method to disaggregate DER electric patterns from aggerated measurements on the LV side of the IEEE European LV Test Feeder. The main differences and new contributions in this research are: (i) greater levels of PV integration are defined in this research, creating a higher volume of DER penetration scenarios in the network; (ii) the consideration of random forest and a multilayer perceptron (MLP) classification methods; (iii) an optimised tuning of machine learning hyperparameters; (iv) the inclusion of statistical variables and variable window size of the electrical records; (v) analysis of three different methodologies including windows, statistical variables and variable window size as inputs of the NILM algorithm; and (vi) a deeper performance evaluation of the NILM method proposed including performance scores, processing times, comparison with other sources and potential contributions to DNO.

The remainder of this paper is organized in nine parts. Section II briefly presents reasons for the lack of observability in conventional LV networks and the effects of increasing DER integration levels. Section III provides a definition of NILM methods. Section IV provides a brief overview of NILM methods focused on DER identification. Section V introduces the methodology and the data preparation techniques. Section VI defines the cases of study and scenarios proposed. Section VII describes the characteristics of the dataset used and the evaluation scenarios proposed including several levels of integration of PV and EV. Section VIII presents a discussion of the results achieved for the identification of DER electrical signatures from aggregated measurements on the LV distribution side of a service transformer using classification approaches. The performance, processing times and a brief comparison of the models with relevant sources are discussed. Section IX draws the summary and conclusions of this work.

II. CHALLENGES OF LV NETWORKS WITH HIGH DER INTEGRATION

Conventionally, electric systems used to have unidirectional power flow from large and centralised power generation plants to supply loads in the customer side. Although customer load demand typically varied based on socio-economic factors, load demand was predictable and utility companies could dimension the network using traditional load forecasting techniques [13]. The information gathered at high and medium voltage was sufficient in conventional electrical networks to manage constraints on LV distribution networks. Thus, distribution networks have conventionally operated without a need of a monitoring infrastructure on the low voltage side [4].

Aggregated after diversity maximum demand (ADMD) projections serve well for planning and load forecasting

at customer levels on conventional networks [14]. The ADMD is conventionally used to dimension network assets and design electric systems based on expected values of maximum customer demand expected after a diversity is applied. However, AMDM estimations do not provide a good representation for the increasing integration of DER load/generation profiles in LV networks. This is due to the significant contribution DER load/generation patterns have in load profiles of a non-DER customer. For example, ADMD values oscillate between 2 and 2.5 kW per customer in Ireland. Yet, low carbon loads such as EV chargers and heat pumps require 7 kW and over 3 kW (or more) respectively [13].

Technologies such as rooftop photovoltaic (PV) systems, small scale wind generation, battery energy storage systems (BESS), among others, cause operational constraints such as overvoltage, power network imbalances and reverse power flow just to mention but a few [15]. Similarly, with the decarbonization of the transport and heating sectors, numbers of low carbon technology loads such as EVs and heat pumps have been rising at the end of the electrical network. This has increased the frequency of power network violation events such as overload, overheating, network asset accelerated ageing, system imbalances and power quality issues, among others [16].

Conventional solutions, such as power curtailment or network reinforcement, increase overall energy prices, causing a higher carbon footprint, but does not maximise the utilization of renewable energy-based assets [17]. This creates a barrier for the rapid and needed decarbonization of power generation, transport, and heating sectors, inhibiting progress towards carbon net zero targets.

III. NON-INTRUSIVE LOAD MONITORING

Non-intrusive load monitoring methods provide a cost-effective solution for DNO to identify in real time the electrical location of DER [18]. These methods are focused on the disaggregation of individual loads from aggregated measurements. Thus, the need to monitor singular electrical appliances at particular sections of the network, known as intrusive load monitoring, is avoided.

Non-intrusive load monitoring reduces the implementation costs, improves scalability but increases the computational complexity of the system. However, current technological advances in software development, data transmission and data storage enable the implementation of NILM methods.

Commonly based on machine learning algorithms, NILM techniques can be classified as supervised and unsupervised methods. Supervised NILM approaches refer to availability of aggregated load records as well as labelled data to train the identification models. Machine learning models such as Random Forest, support vector machines (SVM) and kNN are often used in NILM supervised models. Unsupervised methods study characteristics of aggregated measurements for the identification of clusters of loads, reducing the need for individual labels but lacking the identification of a specific target. As a result, unsupervised methods are generally higher in complexity and methods such as hidden Markov models (and its variations), deep neural networks are frequently used [19].

IV. OVERVIEW OF RELATED WORK

Since NILM methods were introduced by Hart in 1992 [20], research has mainly focused on the assessment of NILM methods for the identification of conventional appliances from electric records behind the meter. As an example, a supervised NILM method was proposed in [21] for the detection of load switching events at customer level. One week of data from the publicly available dataset Building-Level fUlly-labeled dataset for Electricity Disaggregation (BLUED) [22] was used to train and test a random forest classifier. Variable sliding windows, based on average power, were used to identify changes in power consumption of conventional residential loads. A maximum F_1 score of 89.65% was achieved for the event detection. In [23], a NILM method was proposed using a Siamese network, a type of convolutional network. The public datasets PLAID [24] and COOLL [25] were used to obtain V-I trajectory images to train and test the identification model. An F_1 score of 96% was achieved when images of a minimum size of 32×32 pixels were used. Although, NILM methods presented in [21] and [23] provided high performances their main limitation relies on the identification of conventional loads only, which discards variability and stochastic patterns from DER electric profiles.

The identification of DER electrical signatures from aggregated measurements in the residential sector has recently gained more interest from the academic and industrial sectors. Subsequently, a few research studies have developed NILM methods for the identification of individual DER electrical patterns at residential level. In [18] authors proposed a NILM classification method based on time-segmented state probability to identify residential loads. One week of active and reactive power from the 'AMPds' dataset [26] were used as inputs of the algorithm returning an accuracy of over 99% for the identification of an EV load signature. In [27] another NILM method for EV identification was proposed. The approach uses an input data containing active power records of one household for 15 days. Sliding windows of 3 to 5 minutes are used as inputs of the algorithm based on variance and mean absolute deviation to identify EV load profiles. Precision and recall scores of 88% and 93% were achieved. Authors in [28] proposed a NILM method using piecewise aggregate approximation (PAA) and agglomerative clustering for the identification of PV generation patterns. A large dataset of 1,085 houses including 269 PV systems and 104 EV loads were used, achieving an accuracy of 99% for identification of PV systems in term times of weeks, months, and years. One of the main disadvantages of this research is the lack of real time identification, a characteristic required to control DER variable dynamics by DNO. The main limitation of the methods presented in [18], [27],

and [28] is the lower complexity to disaggregate loads at customer level compared to the implementation of load identification techniques at distribution level.

Applied at the LV side of a service transformer, NILM methods contribute to increase the observability of larger areas including greater number of loads and customers. Subsequently, greater complexity is achieved due to the higher presence of conventional loads in a network with comparable low percentages of DER in a distribution network. Although NILM has been widely implemented for the identification of conventional loads (e.g., [27], [28]), a low number of research studies have focused on DER at distribution levels. In [29], a disaggregation method for PV systems power generation from an IEEE 123-node standard test-feeder is developed. The approach evaluates the performance of machine learning algorithms including linear regression, random forest, and a multilayer perceptron. High resolution real dataset from Maui (Hawaii) and a simulated one using GridLab-D were used to train and evaluate the performance of the method proposed using weather, PV generation and aggregated load at the LV side of the service transformer. An R^2 score of 98% was achieved with random forest. The research study concluded that there is lack of pioneer research developing a NILM classification methods for the identification of EVs and PV systems from aggregated measurements on the LV side of a distribution transformer.

Apart from NILM methods, load modelling techniques are frequently used for the power system analysis, planning and control. The main objective of load modelling is to provide a simple, yet accurate, mathematical algorithm to represent a singular or a set of loads [30]. However, the fast and stochastic variability of DER power consumption/generation patterns due to variables such as environmental conditions, consumption patterns, etc., increases the complexity of these models mathematical. Thus, the focus of this work was on supervised NILM methods based on machine learning algorithms capable of learning from individual loads to disaggregate DER electrical patterns in real-time.

V. FRAMEWORK

The NILM method proposed can be outlined into six stages: (i) Data acquisition and interpretation; (ii) Data preprocessing; (iii) Data processing; (iv) Electric profile identification; (v) Assessment; and (vi) Output.

A. DATA ACQUISITION AND INTERPRETATION

Two public data sources are used to simulate the scenarios proposed. First, one year of individual load demand profiles from 55 households are obtained from those available in the IEEE European LV test feeder. Secondly, electric profiles of EV and PV from the public dataset ''Pecan Street – Dataport'' (hereafter called Pecan Street) [31] are used for the purposes of this research. Minutely reported values of EV and PV electric profiles were extracted from 15 households in the Pecan Street dataset for the year of 2017. These residential dwellings, randomly selected from the dataset, had all electric vehicle chargers and 8 of them also included PV generation profiles. Detailed information of the relation of loads, PV systems, EV and their respective power generation/consumption is presented in Table 8 on the Appendix.

TABLE 1. Distribution of loads and DER power in the test feeder selected for the scenario considering 100% EV and 50% PV penetration.

Phase	Demand		PV		EV	
	kW	%	kW_p	%	kW	%
1	112.8	34%	37	40%	97.9	36%
2	127.8	39%	27	29%	112.2	41%
3	89.3	27%	29	31%	63.6	23%
Total	**329.3**		**93**		**273.7**	

B. PRE-PROCESSING

In this stage, PV generation profiles from Pecan Street are normalised per unit (kW/kW peak) to make them adaptable to load profiles in the IEEE European LV test feeder model. Considering EV load profiles are not dependent on a household peak demand, their load profiles are kept as originally found on Pecan Street. Additionally, data wrangling is applied to remove missing values with zeros and clean the dataset from gaps. While aleatory missing samples can be easily handled by machine learning algorithms, data gaps found on the dataset are transformed into an EV disconnected or a PV not generating during a period of time.

Once the data are cleaned, EV and PV profiles were randomly assigned residential houses on the IEEE European LV test feeder to emulate multiple scenarios. In the case of normalised PV peak generation, the PV profiles were set to match the peak demand -kW_p- of the house on the LV network, with PV systems ranging between 1 and 4 kW peak (kW_p). Generation of the PV systems and EV profiles are only added to a particular load when it is required for the simulation of a particular scenario. For instance, with 55 loads in overall connected to the network, only 11 houses will be randomly selected to have either EV or PV under a 20% penetration scenario defined from the numbers of consumers with DER.

Since the number of EV and PV profiles is lower than the houses in the network, the available data were replicated among the 55 houses. Electric profiles of EV and PV systems were carefully allocated to avoid duplicating combinations between these two systems. Therefore, the same ID of EV and PV profiles were not repeated within two houses in the network. As shown in Table 1, the allocation of loads, distributed generation, and EV loads in the electrical circuit, exhibits a clear imbalance with phase 2 having a larger load demand than the other two phases. Similarly, distributed generation and EV loads were added randomly to the distribution network, which is a complex phenomenon driven by factors such as demographic, economic, and geographic aspects, among others [32]. As a result, the phase 1 exhibits the higher level

of PV integration and phase 2 the largest integration of EV for the scenario considering 100% EV and 50% PV penetration.

Load flow at the LV side of the service transformer in the network selected is carried out using the OpenDSS simulation tool and its Python API. Phase values of voltage (V), current (I), real (P) and reactive power (Q) in the transformer were used as inputs for the NILM method. These 4 variables were grouped forming the input matrix (X), containing 1-year data at 1-minute resolution. The ith value of the input matrix X can be represented as $X_i = [P_i, Q_i, V_i, I_i]$.

C. DATA PROCESSING

In this stage, the input matrix X is analysed to contribute to the performance of the machine learning classifiers. Thus, filtering, sliding windows and balancing techniques are applied. First, electric profiles of EV and PV are compared against a threshold value of 100 W to obtain a column vector of Boolean values (y) depicting the presence of each DER at each time t. This contributes to reduce noisy records from the input data from both low carbon technologies. Therefore, if the ith record of a DER is over 100 W the output vector is defined as DER active ($y_i = 1$), while for lower values of the DER is set as inactive ($y_i = 1$). Subsequently, the methodology previously applied at customer level in [33] is replicated on this paper to create windows of aggregated measurements. This contributes to split the data into smaller parts and allows the real time processing. The technique is based in two main variables, namely the window size and the window step. The window size (n) or window width refers to the number of consecutive records stored in a window, while the step (a) indicates the number of samples the next window is shifted to the right. Subsequently, the i^{th} window of size n_x4 is defined as in (1).

$$W_i = [[P_i, \ldots, P_{i+n}], [Q_i, \ldots, Q_{i+n}], [I_i, \ldots, I_{i+n}], [V_i, \ldots, V_{i+n}]] \quad (1)$$

Once the sliding windows are created, the output vector y should be reduced from an $m_x n$ size to a column vector, where m is the number of windows created. In other words, each window should be classified as having or not a DER. For this, if more than half of the active power records were classified as having DER, the window is set as having DER ($y = 1$). Otherwise, the value of y for that window is set to 0.

Due to the normal operation of EV and PV, the input data can be imbalanced regarding electric records including both operation status of a DER (drawing/generating power or disconnected). For example, EVs are usually charged at night for a few hours, but most of the time it is very likely they will be disconnected for most of the day. In the case of a PV system, it will depend on the season, and its generation will vary along the year. Therefore, the data are balanced using the output vector y as a reference. This balancing process consists of comparing the number of windows classified as containing a DER against the ones with only conventional loads (i.e., when the DER is not drawing/generating power). Then, the part presenting the smaller number of windows is kept, while windows of the other part are randomly discarded until the sizes of both groups (DER and non-DER windows) are matched. This creates an even input data (50% DER - 50% non-DER), which contributes to training the machine learning algorithms for a more general scenario and reduces the likelihood of overfitting [34].

D. FEATURE EXTRACTION

As it has been previously presented in [33], statistical variables of sliding windows can contribute to reduce processing times of the classifiers. Therefore, statistical features are extracted from each window W_i for P, Q, V and I. The minimum ($W_{i\,min}$), the maximum ($W_{i\,max}$), the average ($\bar{W}_i$), the distance between minimum and maximum ($W_{i\,max}$- $W_{i\,min}$), the standard deviation (W_σ), the variance (W_σ^2) and the kurtosis (W_k) of each window are computed [35], [36].

$$\bar{W}_i = \Sigma(W_{ijp}) \quad (2)$$

$$W_\sigma^2 = \Sigma(W_{ijp} - \bar{W}_i)/(\mathrm{n} - 1) \quad (3)$$

$$W_\sigma = \mathrm{sqrt}(W_\sigma^2) \quad (4)$$

$$W_k = \mathrm{E}[W_i - \bar{W}_{i,j}]/\sigma^4 \quad (5)$$

where $1 \leq p \leq n$ (window size), $1 \leq j \leq 4$ (standing for P, Q, V and I), and $1 \leq i \leq m$ (number of windows).

E. ELECTRIC PROFILE IDENTIFICATION

Independent classification models are used to identify active power from a DER at the same time. This is two models would be created, one for the identification of EV load profiles and another one for PV systems. In addition, the classification of a DER from the aggregated measurements is proposed to be initially done per phase as first instance. Subsequently, the NILM approach is also evaluated using the combination of windows from all three phases and its performance is provided in the results and discussion sections.

Classification models were developed using conventional machine learning techniques known as kNN, random forest and MLP. The neighbours-based method consists of correlating an unknown sample with its closest or more similar samples, called neighbours, by calculating the shortest/k-shortest Euclidean distance between a new sample and known training ones [9]. Random forest evaluates each sample under multiple structures where each of them are similar to an inverted three to compute the most common answer to make a prediction [10]. The MLP technique simulates the structure of a neuron in the human brain, connecting inputs to layers of neurons, called hidden layers [11]. Each neuron evaluates independently the connections with neurons in previous layers and depending on activation functions the neuron is excited or not. At the end, the MLP decides if the output considering the interactions of all neurons in the system. Back propagation was implemented to adjust and tune connection weights and bias of each neuron. Fundamentals and mathematical

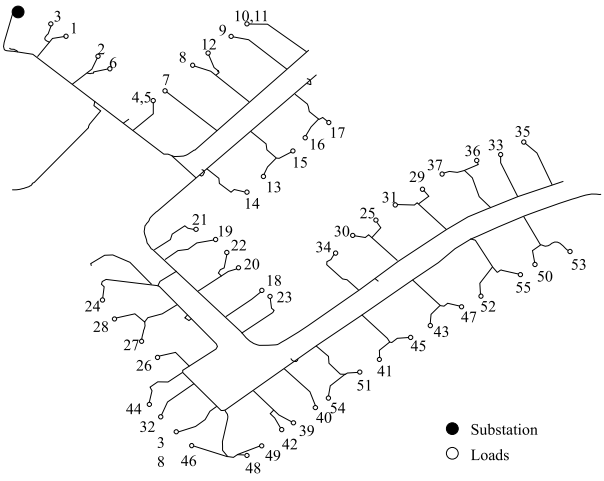

FIGURE 1. IEEE European LV test feeder (reproduced from [38]).

background of the kNN, random forest and MLP techniques can be further investigated in [9], [10], and [11].

F. NILM MODEL ASSESSMENT

Training and test sets are created from the available windows to assess the performance of the machine learning algorithms. Therefore, the entire dataset for each scenario is divided into training and test sets, corresponding to 80% and 20%, respectively. During training, 80% of the windows created from the input matrix X and its correspondent element in the output vector y are used to create a model $f(x)$. The model $f(x)$ is then validated using 20% of unseen data from the input matrix and the predictions are compared with the expected values from the vector y at each timestep t. To provide a comprehensive evaluation of the NILM method proposed, cross-validation with a 5 k-fold is used to reduce possibility of overfitting [34].

To evaluate the performance of the NILM method, classification metrics such as accuracy (A_{CC}), precision (P_r), recall (R_e), and the F_1 score are used [37].

VI. CASE OF STUDY AND SCENARIOS

As a difference from the common 120 V North American LV network with a few customers per transformer, LV networks in Europe typical aggregate several customers in 230 V LV networks. The IEEE European low voltage test feeder presents a radial configuration and a nominal frequency of 50 Hz. A step-down transformer converts the medium voltage at 11 kV to 415 V on the LV side to supply power to 55 households [7]. The single-phase schematic diagram of the IEEE European LV test feeder is illustrated in Fig. 1.

The NILM classification algorithm was assessed under a several EV and PV integration scenarios defined in terms of percentage of customers. For each case, DER are arbitrarily allocated within customer on the LV network. Overall, 100 situations are evaluated in the study which as follows:

- Distributed PV integration: 5% to 50% (5% increment).

TABLE 2. Distributed generation per phase for each simulated scenario.

Scenario PV	Houses with PV	Phase (kW_p) 1	2	3	Generation Capacity (kW_p)
5%	3	7	0	2	9
10%	6	11	0	10	21
15%	8	14	2	10	26
20%	11	21	2	14	37
25%	14	25	2	21	48
30%	17	30	2	25	57
35%	19	33	6	25	64
40%	22	33	12	29	74
45%	25	37	19	29	85
50%	27	37	27	29	93

TABLE 3. Net EV load per phase associated to each simulated scenario.

Scenario EV	EV Owners	Phase (kW) 1	2	3	Net EV load (kW)
10%	6	7.38	15.27	7.3	30.0
20%	11	10.9	31.9	10.	53.5
30%	17	24.0	31.9	14.	70.1
40%	22	37.5	47.8	15.	100.8
50%	27	50.8	47.8	27.	125.7
60%	33	54.2	64.6	33.	152.7
70%	38	64.4	81.5	37.	183.2
80%	44	68.3	98.8	40.	208.0
90%	49	84.8	98.8	52.	236.4
100.0%	55	94.5	112.2	67.	273.7

- Electric vehicles penetration: 10% to 100% (10% increment).

In this case, a 5% increase on DER integration is equivalent to 3 customers (2.75 exactly). Therefore, the maximum PV generation capacity in the network is 93 kW_p and the maximum power required for EV load is 237.7 kWh (if all 55 customers are charging their vehicles simultaneously). A detailed description of the aggregated PV generation and EV load per phase for each of the proposed scenarios is shown in Table 2 and Table 3.

For illustration purposes, per phase values for a 20% EV and PV penetration scenario are exhibited in Fig. 2. As it can be observed, EV charging causes an increase in current, active power and reactive power while PV generation produces the opposite effect. The impact of each DER depends on the infeed transformer demand vs the DER load demand/generation at each time t. Therefore, in the given trends, it can be said that phase 1 had the highest EV power demand and generation on the illustrated day. Similarly, the same day only a few EV were charged at phases 1 and 2 while customers from phase 3 did not charged their vehicles at home.

VII. DER CLASSIFICATION RESULTS

Several set ups including non-balance data (Section V-A), balanced data (Section V-B) and variable sliding windows (Section V-C) are evaluated in this section to provide a clear analysis of the performance of the NILM method proposed. The F_1 score, defined in (4), was initially used to provide

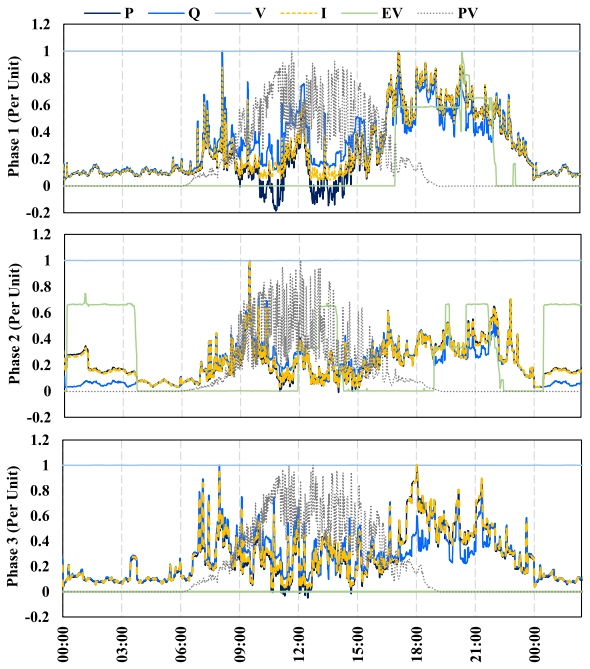

FIGURE 2. Per phase electrical values observed at the LV side of a service transformer in the IEEE European LV test feeder under 20% EV and PV integration in the network. Data for May 19th, 2017.

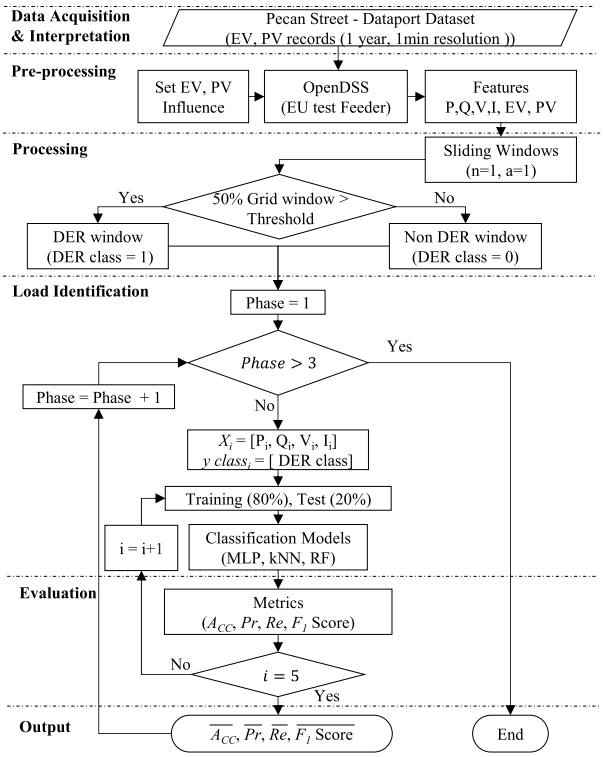

FIGURE 3. Flowchart of a NILM method proposed for the identification of EV and PV electrical signature using individual data from each phase.

a fair overall assessment of the results achieved. Here, the expected value vector was set as a 0 or 1 meaning the presence of a particular DER at each time t. Simulations were performed using Python 3.8.12 and the machine learning library *scikit-learn* (version 1.0.1) on an Intel Core i7-8700 @ 3.20 GHz PC with 16 GB DDR4 RAM. All experiments were run on the same machine to get comparable computational costs. The selection of houses per scenario was completed using a random seed for reproducibility of the experimental results as it is shown in Table 9 for EV and Table 10 for PV.

A. HYPERPARAMETER MODEL SELECTION

Data obtained from the simulation in OpenDSS of the European test feeder is used directly as input of the classifier and each phase is evaluated independently. Windows classified as non-DER and DER windows (i.e., when a DER is not contributing to the aggregated load in a house) are all passed to the classifiers. Minutely reported values of active (P) and reactive power (Q), voltage (V) and current (I) are used to train the NILM models per phase. For this, the output vector (y) is formed comparing the threshold value of 100 W with minutely values of DER power (P_i) to determine if there is a DER influence ($y_i = 1$) or not ($y_i = 0$) among those electrical features. A flow chart of the initial configuration of the proposed NILM method is illustrated in Fig. 3.

A grid search was carried out using the model's topology proposed to determine the best value for the hyperparameters of kNN, RF and MLP. Considering the amount of data involved in the different levels of EV and PV integration, a preliminary experiment was developed for using a small portion of the available data with 3 specific scenarios per DER. Thus, data from scenarios contemplating 10%, 50% and 100% EV influence as well as 10%, 25% and 50% PV were used. Results of simulations carried out for hyperparameter tuning for kNN, RF and MLP are presented in Table 11, Table 12 and Table 13, respectively. A summary of the hyperparameters selected for each machine learning algorithm used in the upcoming stages of the analysis are provided in Table 4.

TABLE 4. Net EV load per phase associated to each simulated scenario.

Method	Parameter	Details
kNN	Neighbours	3
	Weights	Uniform
	Metric	Euclidean
Random Forest	Estimators	100
	Criterion	Gini Impurity
MLP	Hidden layers	3
	Neurons per layer	32
	Optimiser	Adam
	Learning rate	Constant
	Early stop	True
	Activation	ReLU
	EPOCHS (Max.)	500

B. SINGLE PHASE IMBALANCED DATA AS INPUT OF THE CLASSIFICATION MODELS

The process depicted in Section V-A Fig. 3 was used to test the performance of the machine learning models. In total, 100 scenarios defined for the classification of DER electrical

patterns from aggregated measurements are tested. Minutely values of P, Q, V, and I are used directly as inputs for training and testing the machine learning algorithms.

Using fixed hyperparameters for the machine learning algorithms, the performance of the NILM method was evaluated per phase. In general, classification scores for the EV load pattern identification exhibited consistent results among the machine learning techniques. However, performance of the methods proposed varied depending on the phase under analysis. This is because by definition the method proposed observes only one phase at a time, thus translating one scenario into three independent tasks (one per phase). The method also exhibited dependence on the amount of load accumulated on each phase, which made easier for the models to identify EV load profiles in scenarios presenting high influence of EV. Since the allocation of EV owners was done randomly and the power consumption of each vehicle changes among the 15 load profiles used, a better performance was observed in phases 1 and 2 than in phase 3. This is because there were more EVs charged at phase 1 and phase 2.

Once machine learning models were tested, the MLP method was outperformed by kNN and RF. The average training time per sample ($X_i = [P_i, Q_i, V_i, I_i]$) of the MLP method was 244 μs, while its average test time per sample was 2.83 μs. This method provided an F_1 score between 0.70 and 0.84 for around 58% of the evaluated scenarios in the three phases. The kNN method presented average processing times per sample of 1.51 μs and 25.5 μs for training and testing purposes respectively. The neighbours-based method exhibited F_1 scores between 0.71 and 0.83 in 61% of the 300 evaluated scenarios (100 per phase). Better metrics were achieved with RF using the NILM method proposed. In this case, 62% of all simulations reported F_1 score metrics between 0.77 and 0.90 with average processing times of 188 μs and 19.2 μs during training and test respectively. Results of the 900 simulations performed with EV as target of the classification algorithms are summarized in Fig. 4. In this figure, results are summarized per machine learning technique and per each scenario of EV integration (from 10% to 100% in the x axis). It can also be observed the impact of the proposed levels of PV integration in the network on each of the scenarios for EV uptake.

Similarly for PV, MLP metrics were outperformed by kNN and RF. The neural network-based machine learning technique provided F_1 score metrics between 0.87 and 0.97 for 89% of the simulated cases. This method required 231 μs per sample for training and 2.82 μs per sample for testing. With the shortest training times per sample of 1.52 μs and test times of 25.5 μs per sample, kNN outperformed MLP reaching F_1 scores between 0.84 and 0.96 for 76% of the evaluated cases. In the case of RF, the F_1 score was slightly better than the one achieved with kNN. The difference between these two methods was that kNN only reached 0.95 or above F_1 scores for 20% of the cases while for RF more than 53% of the simulated cases reached or surpassed this metric. The RF method presented training and test processing times per sample of 145 μs and 13 μs respectively. Results of the 900 simulations performed with PV as target of the classification algorithms are summarized in Fig. 5. In this figure, it can also be observed the impact of the proposed levels of EV integration in the network on each of the scenarios for PV.

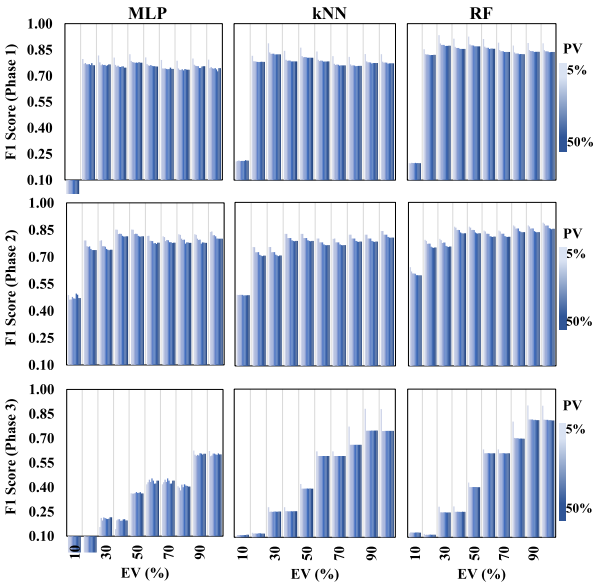

FIGURE 4. Classifier performance as function of EV and PV integration level for the identification of EV demand.

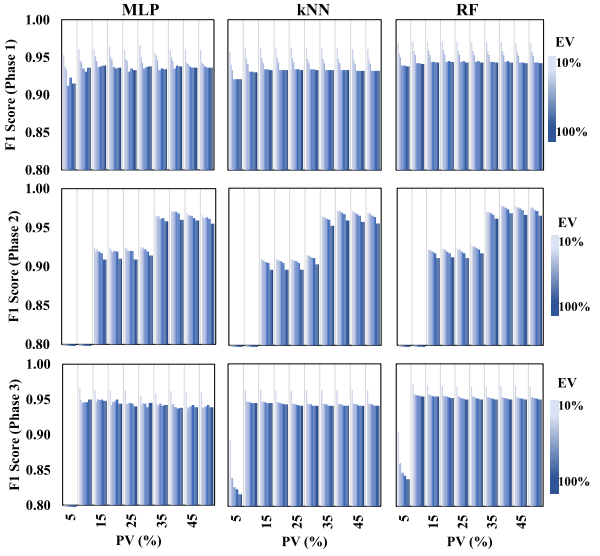

FIGURE 5. Classifier performance as function of EV and PV integration level for the identification of PV generation.

C. MULTI-PHASE BALANCED DATA AS INPUT OF THE CLASSIFICATION MODELS

A disadvantage of the architecture of the NILM method evaluated in Section V-B consists of the assessment of each phase as an individual problem. This leads to having low metrics in a phase where a low level of DER integration is seen while a

phase with high influence of the same DER presents higher classification scores in the same scenario. As an example, see results for EV identification from phase 3 in Fig. 4. This is because the model is trained with imbalanced data, which makes the model good to predict true negative values but lack training to identify true positive ones. Therefore, a second architecture for the NILM method was evaluated concatenating the information from all three phases to get one classification model per DER.

The combination of records from the three phases artificially increments the size of the data from 1 to 3 years (1 year per phase). Thus, the new matrix with columns vectors including P, Q, V, I records from the three phases on the LV side of the distribution transformer are processed to balance the number of samples as previously introduced in Section III-C. For this, the percentage of minutely reported electric variables with DER classified as OFF is compared with the percentage of values on X corresponding to a 1 in the vector of expected values y. Subsequently, the class containing the highest percentage is randomly reduced to match the number of samples on the class with the lower percentage. As a result, the amount of data passed to the machine learning algorithms is optimized using representative values from each of the phases to train the models for both aggregated measurements with and without a DER. Table 5 provides the number of windows obtained with a step size of 1 min to highlight the imbalanced found in the input data. Then, cross-validation is used to present a realistic performance of the NILM methods as shown in Fig. 6.

As a result, the identification of EV load signature provided F_1 score metrics above 0.50 for all the proposed scenarios and machine learning techniques. In the case of MLP, a minimum, average and maximum F_1 score of 0.58, 0.70, and 0.78 were achieved respectively. The most frequent result was found from 0.69 to 0.75, representing 76% of the 100 evaluated scenarios with this method. Similarly, kNN exhibited an average classification metrics of 0.7 for the identification of EV electric load patterns. In total, 90% of the evaluated scenarios provided F_1 scores over 0.64 for kNN with 57% of those results located between 0.69 and 0.73. With a maximum F_1 score of 0.81, this metric presented 26% of the results in the range of 0.73 and 0.77 for the evaluated cases. The minimum F_1 score reached with Random Forest was a 0.02 lower than the one achieved with kNN. However, this machine learning algorithm provided an average F_1 score of 0.73 and 72% of the results were observed between 0.70 and 0.80.

Computational times for the classification of EV load signature were in the order of the μs for both fitting and testing purposes. The results of the 100 simulations carried out for each of the machine learning techniques are presented in Fig. 7. The MLP classifier was the method requiring the largest times per sample to train the model with 314 μs in average. This was followed by RF and kNN which presented computational speeds of 230 μs and 2 μs respectively. In testing, the models greatly reduced their processing times below 30 μs. However, this time kNN was the slowest method, which needed 27 μs per sample in average to make a prediction. Whereas RF needed about 3 μs less than kNN and the MLP model made projections in an average processing time just above 3 μs per sample.

TABLE 5. Number of windows per scenario vs discarded input data.

Approach	DER	Training	Test	Discarded Data
Imbalanced (1 phase)	EV & PV	420,480	105,120	0.0%
Balanced (3 phase)	EV 10%	272,880	68,220	78.4%
	EV 20%	483,976	120,994	61.6%
	EV 30%	655,208	163,802	48.1%
	EV 40%	708,776	177,194	43.8%
	EV 50%	746,064	186,516	40.9%
	EV 60%	766,416	191,604	39.2%
	EV 70%	784,864	196,216	37.8%
	EV 80%	905,808	226,452	28.2%
	EV 90%	996,024	249,006	21.0%
	EV 100%	1,020,712	255,178	19.1%
	PV 5%	667,000	166,750	47.1%
	PV 10%	765,016	191,254	39.4%
	PV 15%	1,081,352	270,338	14.3%
	PV 20%	1,087,288	271,822	13.8%
	PV 25%	1,094,064	273,516	13.3%
	PV 30%	1,100,144	275,036	12.8%
	PV 35%	1,151,528	287,882	8.7%
	PV 40%	1,173,360	293,340	7.0%
	PV 45%	1,180,920	295,230	6.4%
	PV 50%	1,184,776	296,194	6.1%

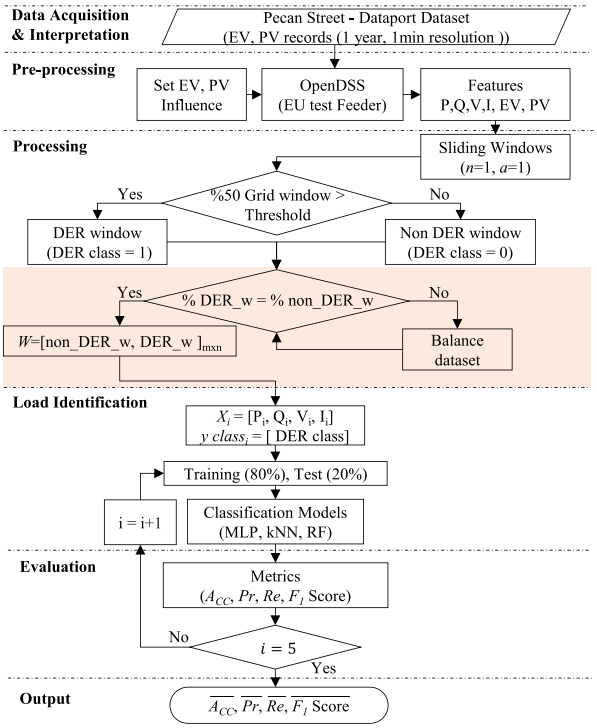

FIGURE 6. Flow chart of a NILM method proposed for the identification of EV and PV electrical signature combining data from the three phases.

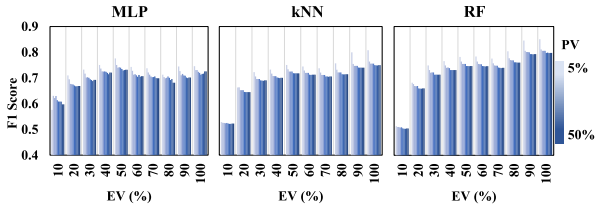

FIGURE 7. Classifier performance for EV identification under several EV integration scenarios.

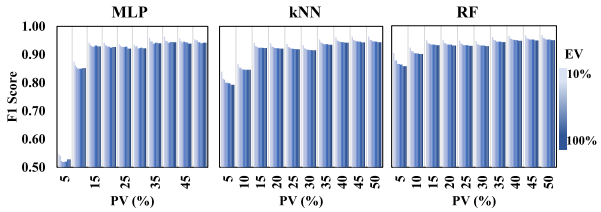

FIGURE 8. Classifier performance for PV identification under several EV integration scenarios.

In the case of PV, F_1 scores were bettered in comparison with the individual assessment of data on each of the phases with regards to the results achieved for the PV identification. The implementation of balanced data from the three-phase system yielded a minimum F_1 score of 0.52, 0.79 and 0.86 for MLP, kNN and RF respectively. In the case of MLP, 80% of the simulations achieved classification metrics between 0.90 and 0.96. The kNN method exhibited a slightly better performance than MLP, achieving F_1 scores from 0.92 to 0.96 in 77% of the evaluated cases. However, Random Forest delivered the best performance among the three methods, reaching F_1 score metrics from 0.92 to 0.97 in 81% of the evaluated cases and at least 10% of these results were higher than 0.95.

In terms of computational speed, the MLP and Random Forest presented processing times of 279 μs and 236 μs for training purposes. This was more than 100 times the time kNN needed to train the system per sample, which was nearly 2 μs. In contrast, kNN presented the highest processing times with 27 μs per sample, while RF and MLP required 21 μs and 3 μs per sample, respectively. The results of the 100 simulations completed for each machine learning technique are summarised in Fig. 8.

D. VARIABLE WINDOW SIZE AND STATISTICAL FEATURES

A third variation of the initial methodology presented in Section V-A is studied. This time, statistical variables of sliding windows were used as inputs of the classifiers as previously proposed in [33]. Electrical features from the three phases were merged on each scenario to avoid issues observed in Section V-B. Subsequently, using the threshold level of 100 W, the vector of 0 and 1 was created to indicate if there was either EV or PV at each time t. The balance data process was also completed to reduce the excess of samples belonging to one class, which leads to higher performance metrics and lower processing times. The balance dataset

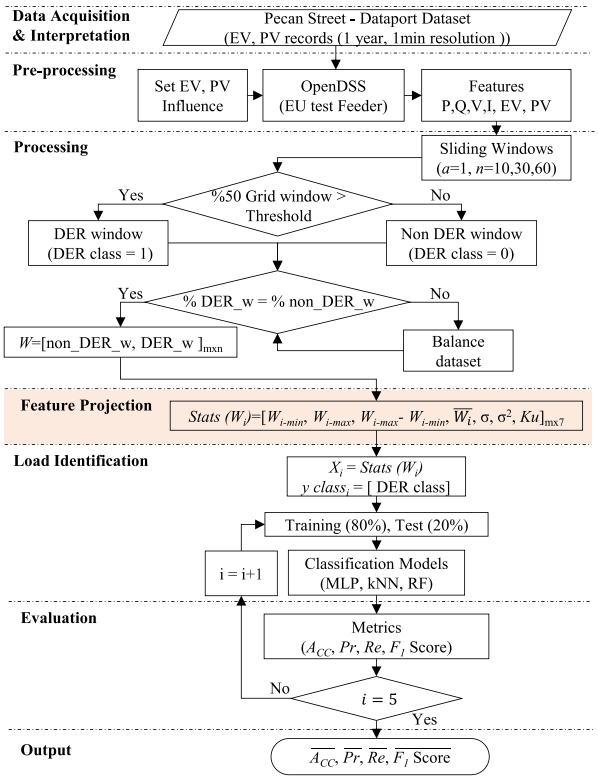

FIGURE 9. Flow chart of the NILM method proposed for the identification of EV and PV electrical signature from windows of active power statistical variables.

containing active power records were grouped into sliding windows of 10 min, 30 min and 60 min. Then, statistical variables of P within the formed windows were used as inputs of the load identification stage as defined in section III-D. Active power was selected in this case because the other three electrical characteristics (Q, V, and I) did not provide relevant information to the model when they were transferred to statistical variables. So, minimum (W_{i-min}), maximum (W_{i-max}), W_{i-max} - W_{i-min}, mean ($\bar{W}_i$), variance (σ^2), standard deviation (σ) and kurtosis (K_u) from each window of active power were used to train and test the NILM model. Consequently, cross-validation is used to evaluate and to present a realistic performance of the NILM methods. The flow chart of this process is shown in Fig. 9.

To analyse the effect of each factor on the identification of a DER, three levels of integration (10%, 50% and 100%) are evaluated against variable window size (10 min, 30 min, 60 min) and variable influence from a different DER (PV if EV or EV if PV). The F_1 score metrics obtained from the implementation of the NILM method proposed on this section for the identification of EV are summarized in Fig. 10.

Regarding the window size, it was observed an inverse relationship between the window width and the performance of the method. Therefore, the window size of 10 min presented the best outcome in all scenarios on each machine learning classifier. In terms of the effect of PV integration, a similar outcome was achieved in the previous sections (V.B and V.C).

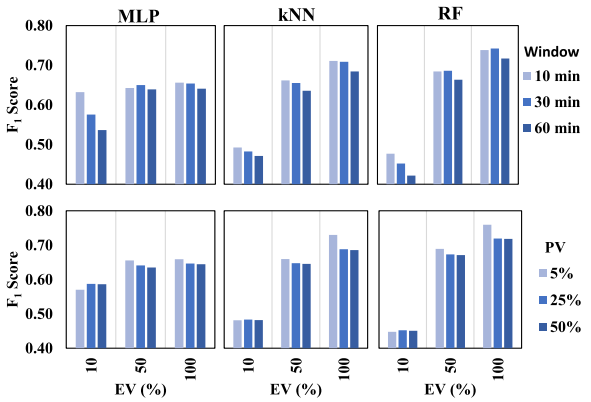

FIGURE 10. Classifier performance using statistical variables of windows of active power for the identification of EV load signatures.

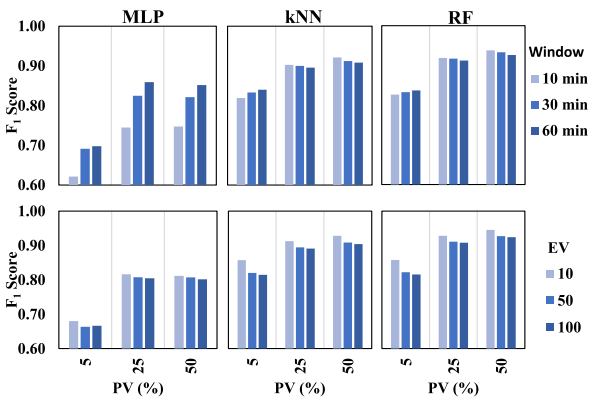

FIGURE 11. Classifier performance using statistical variables of windows of active power for the identification of PV generation profiles.

On those sections, a PV integration below 10% contributed for the machine learning models to provide the best performance scores. Whereas PV integration percentages over 10% contributed to slightly reduce the performance of EV classification due to higher content of noise in the aggregated measurements. This is more visible for the lowest case of PV integration (5%) which yields the best performance metrics for EV identification. The negative effect of the PV integration in the performance metrics of EV classification is less relevant once levels of PV over 25% are integrated. Contrarily, higher number of EV connected to the network contributes to better performance metrics.

One of the biggest differences with respect to the previous modification of the NILM method (using minutely records of $[P, Q, V, I]$ as inputs), relates to the considerable processing time of MLP for training purposes. The implementation of the vector of seven values to train the system, greatly impacted this metrics going from average training times of around 314 μs to 531 μs per sample. In contrast, kNN and RF methods presented similar average processing times during training in comparison with results achieved in Section V-B. Test times per sample were similar to those observed in Section V-B for the three machine learning methods.

Similarly for the identification of PV systems, performance metrics of statistical variables were slightly lower than those achieved with $Xi = [P_i, Q_i, V_i, I_i]$ (minutely records) as inputs. Higher levels of PV also contributed in this case to achieve slightly better performance metrics as illustrated in Fig. 11.

It was observed a small negative impact in the classification of PV generation profiles from increasing levels of EV integration in the network. Regarding window size, the MLP presented a positive relationship with the window width, thus, the larger the window the better the F_1 score. In the case of kNN and RF, a positive increase in metrics was observed with an increase of window size for the 5% PV integration scenario. However, for higher levels of PV integration (25% and 50%), the relationship was inversed, and higher window sizes yielded slightly lower F_1 scores. As it was seen for EV, processing times of kNN and RF were similar as the ones achieved in Section V-B. Yet, the higher number of features used as inputs of the MLP (7 neurons: 7 statistical variables for active power), contributed to an increase of about 47% in training processing times. In this case, the MLP required 477 μs in average per window to train the model.

TABLE 6. Average F_1 score achieved per machine learning method for the identification of EV load profiles at distribution level.

Input Data	Window Size (min)	F_1 Score (%) MLP	kNN	RF
Imbalanced (Phase 1)	1	68.3	73.1	78.8
Imbalanced (Phase 2)	1	76.2	75.1	80.5
Imbalanced (Phase 3)	1	32.4	45.4	47.4
Imbalanced (average)	1	59.0	64.5	68.9
Balanced 3-phase data	1	70.1	69.7	72.7
Balanced 3-phase data (variable window size)	10	64.4	62.2	63.3
	30	62.6	61.5	62.7
	60	60.5	59.7	60.1
Balanced 3-phase data (variable EV)	10	62.5	61.1	62.0

E. SUMMARY OF RESULTS

A summary of the results achieved for the identification of EV load signatures and PV generation profiles from aggregated measurements at LV side are presented in Table 6 and Table 7, respectively. Individual performance and average values of imbalanced data as input (single phase model presented in Section V-B), balanced 3 phase data (multi-phase model, section V-C) and variable window size of statistical features.

VIII. DISCUSSION

The implementation of three main topologies helped to comprehend the effect on both performance and processing times from the data size, quality, hyperparameters of machine learning algorithms, and the models selected.

TABLE 7. Average F_1 score achieved per machine learning method for the identification of PV generation profiles at distribution level.

Input Data	Window Size (min)	F_1 Score (%) MLP	kNN	RF
Imbalanced (Phase 1)	1	93.9	93.7	94.8
Imbalanced (Phase 2)	1	75.2	74.7	75.6
Imbalanced (Phase 3)	1	87.7	93.4	94.4
Imbalanced (average)	1	85.6	87.3	88.2
Balanced 3-phase data	1	88.7	91.3	93.1
Balanced 3-phase data (variable window size)	10	70.4	88.1	89.4
	30	77.9	88.2	89.4
	60	80.3	88.1	89.2
Balanced 3-phase data (variable PV)	10	76.2	88.1	89.3

First, it was observed that balancing the samples per class ($y = 0$ or $y = 1$), contributed to reduced processing times and improved performance scores. Similarly, the usage of the information from the three phases in a scenario of EV and PV integration provides benefits in terms of a larger dataset as input for a one unique model of a particular scenario. This increases the quality of the information passed in the identification stage including higher volume combination between conventional loads and DER in the network. Both the balanced data and the 3-phase data merge contribute to train the machine learning models for more general cases. Moreover, the selection of hyperparameters also played a key role in the trade-off between computational times and performance. For instance, larger number of estimators in RF and greater number of hidden layers in MLP often lead to better performance metrics, but computational costs are increased considerably. Thus, the selection of hyperparameters is essential to balance high performance metrics and fast processing speeds.

When comparing the identification of PV and EV profiles the method presented performed better, and it is more consistent when identifying PV. This may be related to PV presenting a characteristic generation profile, both temporally and between locations, or simply that it is not demand. Electric vehicle might be more difficult to disaggregate as it is closer to conventional large power consuming appliances in the residential sector, such as air conditioning or space and water heating. Additionally, due to the season the data was gathered, larger training data is obtained for PV systems.

A. PERFORMANCE

In general, F_1 score metrics obtained for PV and EV identification from the aggregated measurements on the LV network indicate that the method proposed can provide a reliable identification for both types of DER. The topology of the NILM method presenting the best performance was the one proposed in Section V-B. This model provided homogenous performance for the three phases and the lowest overall processing times for each of the evaluated machine learning techniques.

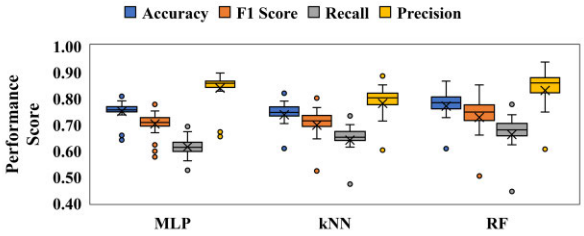

FIGURE 12. Overall classification metrics for EV using balanced data of the three phases to train the machine learning models. For the classification metrics presented, the closer the results are to 1, the best is the performance of the model. Although the classification methods presented similar results, random forest slightly outperform the other two methods.

The highest classification metrics were observed for sensitive levels of integration of the targeted DER and low penetration of the other one. For instance, various integration levels of EV yielded the best metrics when the influence of PV generation was below 10%. Similarly for PV, the best performance metrics were obtained for low levels of integration of EV in the electrical network. However, this impact was not considerable due to it reduced F_1 score about 3.4% and 2% on average for EV and PV, respectively. Therefore, the NILM model proposed can work under the integration of other DER electrical profiles in the network.

The importance of the balanced data is confirmed with the graphical representation of classification metrics such as A_{CC}, P_r, and R_e. Thus, apart from the F_1 score, the other conventional metrics were computed for both EV and PV. The results obtained for the classification of a DER are presented in box plots to summarize the 100 cases evaluated. This is using the balanced dataset of three phases as input of the model proposed and described in Section V-B. Each box plot exhibits percentiles where each error bar represents 25% of the results and the remaining 50% are allocated within the box. The box plot is divided by a line, which indicates the median of the data, and the "X" indicates the average result of each metric. The machine learning models provided similar outcomes for the classification of EV load patterns among other loads in the distribution network as presented in Fig. 12. Excluding outliers illustrated as small dots, average metrics for the identification of EV systems resulted in scores over 0.60. Among the machine learning techniques assessed, RF presented slightly better performance than kNN that also outperformed MLP with corresponding F_1 scores of 0.73, 0.70 and 0.70. Considering the definition of evaluation metrics, the results indicate that the NILM method developed is better at classifying true negative samples than true positive ones. This contributes to obtaining high accuracy and precision, but it does however have a negative impact on the other metrics.

This demonstrates the importance of the F_1 score, which provides a sensible evaluation of the classification process.

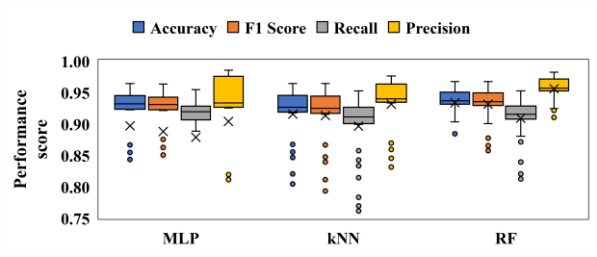

FIGURE 13. Overall classification metrics for PV using balanced data of the three phases to train the machine learning models. Slightly higher performance scores were achieved when random forest was used for the identification of PV systems.

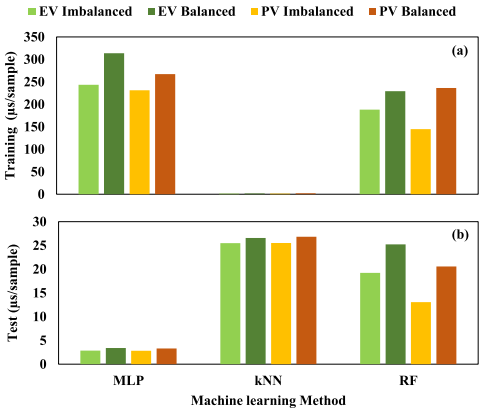

FIGURE 14. Processing times per sample for (a) training and (b) testing of EV and PV identification models.

In the case of PV identification, higher performance scores were achieved, and slightly lower deviations were observed than those in the identification of EV. This means, the results obtained were allocated in smaller ranges. Average results over 90% were obtained in most of the cases, except for precision in the MLP method. The performance of the three models was close to one another, with RF overcoming the kNN and the MLP methods as it was observed in the EV classification approach. The F_1 score was in this case 0.93, 0.91, and 0.89 for RF, kNN and MLP respectively. The effect of the balanced data can be also observed in this case with consistent performance metrics providing relatively close results in all three models. The results for PV identification are summarized in Fig. 13.

B. PROCESSING TIMES

In Fig. 14 (a) average processing times for training purposes are summarized per machine learning algorithm, type of data and DER. From this graph it can be said that in general the DER does not have a considerable impact on the computational effort to process each sample. However, a slight increase per sample from the implementation of imbalanced data to the balanced one was observed. Although, this is certainly true if one compares processing times per sample, the smaller size of a balanced dataset contributes to reduced simulation speeds.

In terms of the machine learning algorithms, MLP presented the higher processing times per sample with computational speeds between 314 μs and 231 μs. Random Forest outperformed these times with speeds between 236 μs and 145 μs. The neighbour-based method outperformed this processing times in training stages needing only up to 2 μs per sample. As it is exhibited in Fig. 14 (b), a different outcome was observed in terms of processing times for testing purposes regarding the computational effort required for each machine learning algorithm to process each sample. In this case, the MLP method outperformed both RF and kNN, which presented scoring times of up to 3.1 μs per sample. Random Forest also provided lower times for testing than it did for training, with scoring times in the range of 13 μs to 25 μs. Not surprisingly, kNN required the longest computational effort to make a prediction with 26 μs in average.

C. COMPARISON WITH OTHER SOURCES

The method proposed can be compared to other research studies in the literature for the identification of PV systems. A NILM method based on statistical features and sliding windows was presented in [35] using high frequency reporting rates recorded with an OpenPMU instrument [39]. Overall, classification metrics over 0.95 were achieved. Similarly, an unsupervised NILM based in agglomerative clustering was presented in [28] with an overall accuracy of 0.95 in the evaluated periods. Therefore, performance metrics achieved in Section V for the identification of PV generation are in range with recent research studies available in the literature.

The identification of EV systems from aggregated measurements has been analysed in the literature. In the residential sector a real-time classification method based on principal component analysis and random forest was presented in [40] to disaggregate EV loads, reaching metrics over 0.92. An event based NILM method for the identification of EV and air-conditioning systems was developed in [27] with precision and recall metrics that projected scores over 0.6 when analysing several scenarios for their parameter configuration. An unsupervised NILM method was proposed in [41] for the identification of different charging stages of several EV with overall metrics for P_r, R_e and F_1 score over 0.89. Considering these studies in the literature, the method based on RF as the classification algorithm provides slightly lower metrics than previous research studies, with an overall F_1 score of 0.73 for the scenarios evaluated. Therefore, further work is needed to achieve better EV identification.

The studies mentioned in [28] and [35], for PV and in [27], [40], and [41] for EV classification were developed at single customer level, considerably reducing the complexity of load profile disaggregation. The method presented in this paper focused on a large group of customers or service area, which increased the complexity of the problem but also the application of the solution.

D. POTENTIAL CONTRIBUTIONS TO DNO

Globally distribution network operators are investigating the deployment of LV monitors. For example, Western Power Distribution (WPD) and UK Power Networks (UKPN), two DNO in the UK, presented outcomes of the technological study of LV monitors to increase the visibility in the UK LV networks. The project LV sensors [42] provided relevant learnings for the development of safe installation policies on working in substations without interrupting customer supply. These projects provide a faster approach to effectively reach a better map of the LV distribution side, complementing the slow transition from conventional metering devices to smart meters at customer levels. Yet, to date the focus has been placed into monitoring network conditions and fault identification but not active identification of DER on the LV network.

The identification of DER in the distribution network is key for the future operation of the electrical system and the transition from fossil fuel based economic sectors such as transport and heating to more sustainable ones. The lack of updated records of DER at LV levels enlarges technical issues due to their fast and variable dynamics. Thus, DNO are driven to implement less efficient investments in the network infrastructure such as conventional infrastructure reinforcement.

The use of NILM methods for the real time DER identification at the LV side of a distribution transformer provides benefits that can be grouped into technical, economic, social, and environmental [43]. First, active identification and localisation of DER contributes to enhanced network planning and operation. The identification of critical sections of the network, with large percentages of DER enables DNO, to implement innovative techniques such as flexibility and active load management. It also informs investment decisions for critical network infrastructure, supported by better DER uptake projections and network capacity. As a result, better DER allocation can be achieved with reduced network constraints and more effective control strategies, increasing LV networks flexibility and resilience.

A better utilization of electrical network assets contributes to efficient network investments, benefiting all electrical network stakeholders. For DNO, better network maps enable predictive and preventive maintenance instead of reactive maintenance. This reduces reparation costs and contributes to a better utilization of personnel. It has also been demonstrated that NILM methods contribute to energy savings for customers [1]. This combined with participation on variable pricing schemes contributes to reducing customer energy bills.

The real time identification of DER on the LV network increases the reliability of the electrical system. Consequently, power outages can be reduced and with more efficient network interventions the quality of the electric system can be improved. The location of DER also enables DNO to implement solutions to reduce energy poverty and promote a fair energy service. Thus, avoiding innovation and reinforcement costs to customers without a DER.

TABLE 8. Relation of loads with EV, PV, and location in the network.

Load	Peak Load (kW)	Phase	PV generation Capacity		EV load	
			House ID	kW_p	House ID	kW
1	2.77	1	370	3	1202	6.6
2	3.55	2	2638	4	1953	3.4
3	8.31	1	3368	4	4998	3.5
4	5.18	1	4526	4	5809	3.4
5	3.44	1	5749	3	6910	3.9
6	2.41	2	7024	2	9609	3.4
7	14.6	2	8197	4	370	3.4
8	8.97	3	9647	4	2638	8.4
9	6.84	1	370	4	3368	1.4
10	5.41	2	2638	4	4526	3.4
11	2.31	2	3368	2	5749	6.0
12	2.23	3	4526	2	7024	3.3
13	9.24	2	5749	4	8197	7.3
14	2.47	1	7024	2	9647	9.6
15	3.10	2	8197	3	9935	9.9
16	8.83	3	9647	4	1202	6.6
17	2.74	3	370	3	1953	3.4
18	11.1	3	2638	4	4998	3.5
19	9.65	3	3368	4	5809	3.4
20	6.22	1	4526	4	6910	3.9
21	3.07	1	5749	3	9609	3.4
22	1.83	1	7024	2	370	3.4
23	9.52	2	8197	4	2638	8.4
24	9.09	3	9647	4	3368	1.4
25	3.32	1	370	3	4526	3.4
26	12.6	2	2638	4	5749	6.0
27	8.13	3	3368	4	7024	3.3
28	0.79	3	4526	1	8197	7.3
29	10.5	1	5749	4	9647	9.6
30	3.04	1	7024	3	9935	9.9
31	8.30	1	8197	4	1202	6.6
32	5.72	3	9647	4	1953	3.4
33	9.79	3	370	4	4998	3.5
34	8.57	1	2638	4	5809	3.4
35	10.5	2	3368	4	6910	3.9
36	2.75	2	4526	3	9609	3.4
37	4.98	2	5749	4	370	3.4
38	12.2	2	7024	4	2638	8.4
39	3.10	3	8197	3	3368	1.4
40	3.48	2	9647	3	4526	3.4
41	2.18	2	370	2	5749	6.0
42	5.07	3	2638	4	7024	3.3
43	2.28	3	3368	2	8197	7.3
44	2.83	2	4526	3	9647	9.6
45	12.2	2	5749	4	9935	9.9
46	7.84	1	7024	4	1202	6.6
47	1.73	3	8197	2	1953	3.4
48	8.89	1	9647	4	4998	3.5
49	3.49	1	370	3	5809	3.4
50	2.97	2	2638	3	6910	3.9
51	3.57	1	3368	4	9609	3.4
52	8.27	1	4526	4	370	3.4
53	10.7	2	5749	4	2638	8.4
54	3.30	1	7024	3	3368	1.4
55	2.90	1	8197	3	4526	3.4

* House ID on Table A.I relates to Pecan Street – Dataport Dataset

In the end, all the mentioned benefits achieved at utility and customer level, contribute to a reduced carbon footprint for the electrical system. The optimization of electrical network assets, promoting a higher integration of low carbon loads and distributed generation on the LV network, provides a better utilization of available renewable energy resources. This goes in line with current global targets to achieve carbon net zero by 2050.

E. LIMITATIONS

The input data proposes challenges to the NILM method for the identification of PV electrical generation patterns and

TABLE 9. Houses with EV in the LV network per scenario.

Scenario EV	EV Owners	House ID (IEEE European LV Voltage test feeder)
10%	6	10,20,23,40,43,51
20%	11	3,6,32,37,44
30%	17	9,22,42,49,54,55
40%	22	15,30,39,41,48
50%	27	1,16,24,27,31
60%	33	4,7,12,36,45,47
70%	38	32,38,46,52,53
80%	44	2,5,11,33,35,50
90%	49	8,19,25,29,34
100%	55	13,14,17,18,26,28

TABLE 10. Houses with PV in the LV network per scenario.

Scenario PV	Houses with PV	House ID (IEEE European LV Voltage test feeder)
5%	3	54, 51, 43
10%	6	9, 27, 8
15%	8	25, 41
20%	11	20, 49, 24
25%	14	46, 39, 42
30%	17	30, 18, 22
35%	19	5, 2
40%	22	16, 15, 40
45%	25	29, 36, 10
50%	27	38, 53

TABLE 11. Hyperparameter grid search for kNN as classification method.

Scenario			Results for EV			Results for PV		
% PV	% EV	Phase	F_1 (k_b)	Best k	F_1 (Best k)	F_1 (k_b)	Best k	F_1 (Best k)
5	10	1	0.2	1	0.23	0.9	3	0.96
5	10	2	0.4	5	0.50	0.0	1	0.00
5	10	3	0.1	1	0.13	0.8	1	0.90
5	50	1	0.8	5	0.86	0.9	5	0.92
5	50	2	0.8	14	0.85	0.0	1	0.00
5	50	3	0.4	3	0.42	0.8	1	0.83
5	100	1	0.8	2	0.83	0.9	5	0.92
5	100	2	0.8	6	0.85	0.0	1	0.00
5	100	3	0.8	1	0.88	0.8	1	0.82
25	10	1	0.2	1	0.23	0.9	3	0.96
25	10	2	0.4	7	0.50	0.9	21	0.92
25	10	3	0.1	1	0.14	0.9	3	0.96
25	50	1	0.8	4	0.81	0.9	5	0.93
25	50	2	0.8	12	0.82	0.9	21	0.91
25	50	3	0.4	7	0.40	0.9	3	0.94
25	100	1	0.7	2	0.78	0.9	5	0.93
25	100	2	0.8	4	0.83	0.9	13	0.90
25	100	3	0.7	1	0.75	0.9	3	0.94
50	10	1	0.2	1	0.23	0.9	3	0.96
50	10	2	0.4	9	0.50	0.9	3	0.97
50	10	3	0.1	1	0.14	0.9	3	0.96
50	50	1	0.8	4	0.81	0.9	5	0.93
50	50	2	0.7	16	0.81	0.9	3	0.97
50	50	3	0.4	9	0.40	0.9	3	0.94
50	100	1	0.7	2	0.78	0.9	5	0.93
50	100	2	0.8	2	0.81	0.9	3	0.96
50	100	3	0.7	1	0.75	0.9	3	0.94

reduces the complexity for the model to disaggregate EV load profiles. In the case of PV, peak demand of a house will determine the peak generation of a particular PV system.

TABLE 12. Hyperparameter grid search for RF as classification method.

Scenario			Results for EV			Results for PV		
% PV	% EV	Phase	F_1 (r_b)	Best r	F_1 (Best r)	F_1 (r_b)	Best r	F_1 (Best r)
5	10	1	0.20	25	0.20	0.97	125	0.97
5	10	2	0.64	75	0.64	0.00	25	0.00
5	10	3	0.13	50	0.13	0.90	125	0.90
5	50	1	0.93	125	0.93	0.94	75	0.94
5	50	2	0.87	50	0.87	0.00	25	0.00
5	50	3	0.43	125	0.44	0.85	100	0.85
5	100	1	0.89	125	0.89	0.94	125	0.94
5	100	2	0.89	125	0.89	0.00	25	0.00
5	100	3	0.90	125	0.90	0.84	125	0.84
25	10	1	0.20	25	0.20	0.97	125	0.97
25	10	2	0.61	125	0.61	0.92	125	0.92
25	10	3	0.13	50	0.13	0.97	100	0.97
25	50	1	0.87	100	0.88	0.94	125	0.94
25	50	2	0.85	125	0.85	0.92	125	0.92
25	50	3	0.41	125	0.41	0.95	125	0.95
25	100	1	0.84	100	0.84	0.94	125	0.94
25	100	2	0.87	75	0.87	0.91	125	0.91
25	100	3	0.81	125	0.81	0.95	125	0.95
50	10	1	0.20	25	0.20	0.97	125	0.97
50	10	2	0.60	125	0.60	0.98	75	0.98
50	10	3	0.13	25	0.13	0.97	125	0.97
50	50	1	0.87	125	0.87	0.94	125	0.94
50	50	2	0.83	125	0.83	0.97	125	0.97
50	50	3	0.40	75	0.41	0.95	125	0.95
50	100	1	0.84	125	0.84	0.94	125	0.94
50	100	2	0.86	125	0.86	0.97	125	0.97
50	100	3	0.81	125	0.81	0.95	125	0.95

TABLE 13. Hyperparameter grid search for MLP as classification method.

Scenario			Results for EV			Results for PV		
% PV	% EV	Phase	F_1 ($ML P_b$)	Best MLP	F_1 (Best MLP)	F_1 ($ML P_b$)	Best MLP	F_1 (Best MLP)
5	10	1	0.00	1x32	0.00	0.92	2x64	0.96
5	10	2	0.20	3x32	0.49	0.00	1x32	0.00
5	10	3	0.00	1x32	0.00	0.22	3x32	0.30
5	50	1	0.79	3x32	0.82	0.87	2x64	0.92
5	50	2	0.84	3x32	0.85	0.00	1x32	0.00
5	50	3	0.37	2x32	0.38	0.18	64x6	0.28
5	10	1	0.77	3x32	0.79	0.87	2x64	0.92
5	10	2	0.83	2x32	0.84	0.00	1x32	0.00
5	10	3	0.58	3x32	0.62	0.13	2x64	0.26
25	10	1	0.00	1x10	0.00	0.94	2x32	0.96
25	10	2	0.12	3x32	0.47	0.91	2x64	0.92
25	10	3	0.00	1x32	0.00	0.94	3x32	0.96
25	50	1	0.73	2x64	0.77	0.90	2x32	0.94
25	50	2	0.82	2x64	0.83	0.91	2x64	0.92
25	50	3	0.37	3x32	0.37	0.92	3x32	0.95
25	10	1	0.72	2x32	0.74	0.90	2x64	0.94
25	10	2	0.81	3x32	0.82	0.89	2x64	0.91
25	10	3	0.58	3x32	0.61	0.93	2x32	0.94
50	10	1	0.00	2x64	0.00	0.94	2x64	0.96
50	10	2	0.15	3x32	0.47	0.94	2x64	0.97
50	10	3	0.00	(32)	0.00	0.93	3x32	0.96
50	50	1	0.72	3x32	0.78	0.90	3x32	0.94
50	50	2	0.81	3x32	0.82	0.94	3x32	0.96
50	50	3	0.37	(100)	0.37	0.92	3x32	0.94
50	10	1	0.72	3x32	0.74	0.90	2x64	0.94
50	10	2	0.79	3x32	0.80	0.91	3x32	0.96
50	10	3	0.58	3x32	0.60	0.92	2x64	0.94

Thus, one PV system can have smaller or larger peak generation depending on the maximum power consumption of a particular household. For example, the PV system with ID 370 used for houses 1 and 9 will have a peak demand of

3 kWp and 4 kWp respectively. The integration of a different EV to each house also increases the variability of the data for the NILM model to disaggregate PV generation profiles. In the case of EV classification, the integration of the original EV load profiles reduces the variability of the data when the NILM model aims to disaggregate EV power consumption from aggregated measurements. To avoid overfitting identification models, the integration of PV generation with high variability combined with different household load profiles, contributes to minimise the lack of enough independent EV electrical patterns.

This highlights the importance of establishing collaboration projects between academia and industry. This could contribute providing large datasets to train and test NILM models. Additionally, machine learning algorithms could learn specific customer patterns of focus areas (such as a city, a country) leading to improve performance metrics of NILM methods. Thus, performance metrics of NILM could be improved.

IX. CONCLUSION

The aim of this work was to propose a NILM method based on conventional machine learning algorithms such as kNN and RF. Additionally, a multilayer perceptron was also used to analyse its performance for classification purposes. Three topologies of the NILM method proposed were evaluated and results of 2,724 simulations were analysed. The supervised NILM method was tested for the detection of DER electrical patterns under several penetration scenarios of EV and PV systems during 1-year of data at 1 min reporting rates. A considerably higher performance was achieved for the identification of EV load profiles (average F_1 score of 0.73) and PV systems (average F_1 score above 0.93). This was obtained using balanced data of the three phases of the distribution transformer as inputs of the classifiers. Considering reporting rates defined for monitoring infrastructure in secondary substations at distribution levels, the results achieved under 314 μs confirm the feasibility to implement the methodology proposed for real-time identification of DER.

The metrics obtained in the application of the NILM methods on the LV side of distribution transformers relate to those presented in previous literature and serve as a base line for future methods aiming for higher performance scores. In the case of PV systems identification, metrics exceeded the range of previous literature applied at household level (e.g., $F_1 = 92\%$ in [35]). Thus, proving outstanding performance for PV identification. Further improvements are however needed to increase performance of the models proposed for both DER but specifically for EV identification. The work can be expanded in the future to evaluate regression models and predict load demand/generation from a specific DER in the LV network.

All in all, the high results suggest that the NILM method proposed is valid for the purpose of identifying DER (e.g., EV and PV systems) in power networks serving a group of customers in the residential sector. Thus, the method could be replicated by distribution network operators to increase the observability of LV distribution networks. This contributes to more efficient planning and operation of LV networks, enhanced control systems, optimised network investments, and maximises the usage of renewable energy resources towards the decarbonization of the electrical system.

APPENDIX

See Tables 8–13.

ACKNOWLEDGMENT

The authors would like to thank Pecan Street Inc. for making freely available the energy data from DER systems for this research work. Data sharing is not applicable to this article as no new data were created or analysed in this study. The input data used in this study are available in the IEEE European LV Voltage test feeder model and The Pecan Street - Dataport Dataset at https://www.pecanstreet.org/.

REFERENCES

[1] R. Liaqat, I. A. Sajjad, M. Waseem, and H. H. Alhelou, "Appliance level energy characterization of residential electricity demand: Prospects, challenges and recommendations," *IEEE Access*, vol. 9, pp. 148676–148697, 2021, doi: 10.1109/ACCESS.2021.3123196.

[2] A. E. Auld, J. Brouwer, and G. S. Samuelsen, "Analysis and visualization method for understanding the voltage effect of distributed energy resources on the electric power system," *Electric Power Syst. Res.*, vol. 82, no. 1, pp. 44–53, Jan. 2012, doi: 10.1016/j.epsr.2011.08.012.

[3] W. Chen, Y. Ma, and C. Bai, "The impact of carbon emission quota allocation regulations on the investment of low-carbon technology in electric power industry under peak-valley price policy," *IEEE Trans. Eng. Manag.*, early access, Nov. 18, 2022, doi: 10.1109/TEM.2021.3121002.

[4] M. Markovic, A. Sajadi, A. Florita, R. Cruickshank III, and B.-M. Hodge, "Voltage estimation in low-voltage distribution grids with distributed energy resources," *IEEE Trans. Sustain. Energy*, vol. 12, no. 3, pp. 1640–1650, Jul. 2021, doi: 10.1109/TSTE.2021.3060546.

[5] H. Laaksonen, C. Parthasarathy, H. Khajeh, M. Shafie-Khah, and N. Hatziargyriou, "Flexibility services provision by frequency-dependent control of on-load tap-changer and distributed energy resources," *IEEE Access*, vol. 9, pp. 45587–45599, 2021, doi: 10.1109/ACCESS.2021.3067297.

[6] C. Garcia-Santacruz, A. Marano-Marcolini, and J. L. Martinez-Ramos, "Optimal location of distributed energy resources considering investment costs, use of resources and network constraints," *IEEE Access*, vol. 9, pp. 163379–163390, 2021, doi: 10.1109/ACCESS.2021.3133438.

[7] K. P. Schneider et al., "Analytic considerations and design basis for the IEEE distribution test feeders," *IEEE Trans. Power Syst.*, vol. 33, no. 3, pp. 3181–3188, Oct. 2017, doi: 10.1109/TPWRS.2017.2760011.

[8] Electric Power Research Institute (EPRI). Simulation Tool—OpenDSS. Smart Grid Resource Center. Accessed: Apr. 1, 2021. [Online]. Available: https://smartgrid.epri.com/SimulationTool.aspx

[9] T. Hastie, R. Tibshirani, and J. Friedman, *The Elements of Statistical Learning: Data Mining, Inference, and Prediction*, vol. 27, no. 2, 2nd ed. New York, NY, USA: Springer, 2009. [Online]. Available: http://www.springerlink.com/index/D7X7KX6772HQ2135.pdf

[10] A. Géron, *Hands-On Machine Learning With Scikit-Learn, Keras and TensorFlow*, 2nd ed. Sebastopol, CA, USA: O'Reilly Media, 2019, doi: 10.1201/9780367816377.

[11] S. Skansi, *Introduction to Deep Learning: From Logical Calculus to Artificial Intelligence*. Zagreb, Croatia: Springer, 2018, doi: 10.1007/978-3-319-73004-2.

[12] A. F. M. Jaramillo, J. L. Lorente, D. Laverty, J. M. del Rincon, and A. M. Foley, "Identification of distributed energy resources in low voltage distribution networks," in *Proc. IEEE PES Innov. Smart Grid Technol. Eur. (ISGT Europe)*, Oct. 2021, pp. 1–6, doi: 10.1109/ISGTEurope52324.2021.9639971.

[13] A. Walsh, "Doubling the ADMD in housing schemes to cater for future electrification of heat and transport," in *Proc. CIRED Porto Workshop, E-Mobility Power Distribution Syst.*, 2022, pp. 28–32, doi: 10.1049/icp.2022.0655.

[14] L. F. Ochoa and P. Mancarella, "Low-carbon LV networks: Challenges for planning and operation," in *Proc. IEEE Power Energy Soc. Gen. Meeting*, Jul. 2012, pp. 14–15, doi: 10.1109/PESGM.2012.6344760.
[15] J. Lopez-Lorente, X. A. Liu, R. J. Best, G. Makrides, and D. J. Morrow, "Techno-economic assessment of grid-level battery energy storage supporting distributed photovoltaic power," *IEEE Access*, vol. 9, pp. 146256–146280, 2021, doi: 10.1109/ACCESS.2021.3119436.
[16] M. Al-Muhaini, "Electric vehicle Markov-based adequacy modeling for electric microgrids," *IEEE Access*, vol. 8, pp. 132721–132735, 2020, doi: 10.1109/ACCESS.2020.3010614.
[17] X. Xu, J. Li, Z. Xu, J. Zhao, and C. S. Lai, "Enhancing photovoltaic hosting capacity—A stochastic approach to optimal planning of static VAR compensator devices in distribution networks," *Appl. Energy*, vol. 238, pp. 952–962, Mar. 2019, doi: 10.1016/j.apenergy.2019.01.135.
[18] L. Liu, F. Li, Z. Cheng, Y. Zhou, J. Shen, R. Li, and S. Xiong, "Non-intrusive load monitoring method considering the time-segmented state probability," *IEEE Access*, vol. 10, pp. 39627–39637, 2022, doi: 10.1109/ACCESS.2022.3167132.
[19] A. F. M. Jaramillo, D. M. Laverty, D. J. Morrow, J. M. del Rincon, and A. M. Foley, "Load modelling and non-intrusive load monitoring to integrate distributed energy resources in low and medium voltage networks," *Renew. Energy*, vol. 179, pp. 445–466, Dec. 2021, doi: 10.1016/j.renene.2021.07.056.
[20] G. W. Hart, "Nonintrusive appliance load monitoring," *Proc. IEEE*, vol. 80, no. 12, pp. 1870–1891, Dec. 1992, doi: 10.1109/5.192069.
[21] P. R. Z. Taveira, C. H. V. De Moraes, and G. Lambert-Torres, "Non-intrusive identification of loads by random forest and fireworks optimization," *IEEE Access*, vol. 8, pp. 75060–75072, 2020, doi: 10.1109/ACCESS.2020.2988366.
[22] K. Anderson, A. Ocneanu, D. Benitez, D. Carlson, A. Rowe, and M. Berges, "Blued: A fully labeled public dataset for event-based non-intrusive load monitoring research," in *Proc. 2nd KDD Workshop Data Mining Appl. Sustainability*, Beijing, China, 2012, pp. 12–16.
[23] M. Yu, B. Wang, L. Lu, Z. Bao, and D. Qi, "Non-intrusive adaptive load identification based on Siamese network," *IEEE Access*, vol. 10, pp. 11564–11573, 2022, doi: 10.1109/ACCESS.2022.3145982.
[24] R. Medico, L. De Baets, J. Gao, S. Giri, E. Kara, T. Dhaene, C. Develder, M. Bergés, and D. Deschrijver, "A voltage and current measurement dataset for plug load appliance identification in households," *Sci. Data*, vol. 7, no. 1, pp. 1–10, Feb. 2020, doi: 10.1038/s41597-020-0389-7.
[25] T. Picon, M. Nait Meziane, P. Ravier, G. Lamarque, C. Novello, J.-C. Le Bunetel, and Y. Raingeaud, "COOLL: Controlled on/off loads library, a public dataset of high-sampled electrical signals for appliance identification," 2016, *arXiv:1611.05803*.
[26] S. Makonin, B. Ellert, I. V. Bajić, and F. Popowich, "Electricity, water, and natural gas consumption of a residential house in Canada from 2012 to 2014," *Sci. Data*, vol. 3, no. 1, pp. 1–12, 2016, doi: 10.1038/sdata.2016.37.
[27] A. U. Rehman, T. T. Lie, B. Valles, and S. R. Tito, "Event-detection algorithms for low sampling nonintrusive load monitoring systems based on low complexity statistical features," *IEEE Trans. Instrum. Meas.*, vol. 69, no. 3, pp. 751–759, Mar. 2020, doi: 10.1109/TIM.2019.2904351.
[28] D. L. Donaldson and D. Jayaweera, "Effective solar prosumer identification using net smart meter data," *Int. J. Electr. Power Energy Syst.*, vol. 118, Jun. 2020, Art. no. 105823, doi: 10.1016/j.ijepes.2020.105823.
[29] R. Saeedi, S. K. Sadanandan, A. K. Srivastava, K. L. Davies, and A. H. Gebremedhin, "An adaptive machine learning framework for behind-the-meter load/PV disaggregation," *IEEE Trans. Ind. Informat.*, vol. 17, no. 10, pp. 7060–7069, Oct. 2021, doi: 10.1109/TII.2021.3060898.
[30] A. Arif, Z. Wang, J. Wang, B. Mather, H. Bashualdo, and D. Zhao, "Load modeling—A review," *IEEE Trans. Smart Grid*, vol. 9, no. 6, pp. 5986–5999, Nov. 2018, doi: 10.1109/TSG.2017.2700436.
[31] Pecan Street Inc. *Pecan Street Dataport*. Accessed: Jul. 1, 2021. [Online]. Available: https://www.pecanstreet.org/
[32] *Electric Vehicle Uptake Modelling (EV-Up)*, ENA Smarter Netw. Portal, Energy Netw. Assoc. (ENA), London, U.K., Accessed: May 14, 2022. [Online]. Available: https://www.spenergynetworks.co.uk/userfiles/file/EV-Up_NIA_project_closedown_report.pdf
[33] A. F. Moreno Jaramillo, J. Lopez-Lorente, D. M. Laverty, J. Martinez-del-Rincon, D. J. Morrow, and A. M. Foley, "Effective identification of distributed energy resources using smart meter net-demand data," *IET Smart Grid*, vol. 5, no. 2, pp. 120–135, Apr. 2022, doi: 10.1049/stg2.12056.
[34] J. D. Domingo, R. M. Aparicio, and L. M. G. Rodrigo, "Cross validation voting for improving CNN classification in grocery products," *IEEE Access*, vol. 10, pp. 20913–20925, 2022, doi: 10.1109/ACCESS.2022.3152224.
[35] A. F. M. Jaramillo, D. M. Laverty, J. M. del Rincon, P. Brogan, and D. J. Morrow, "Non-intrusive load monitoring algorithm for PV identification in the residential sector," in *Proc. 31st Irish Signals Syst. Conf. (ISSC)*, Jun. 2020, pp. 1–6, doi: 10.1109/ISSC49989.2020.9180192.
[36] S. Raurale, J. McAllister, and J. M. del Rincon, "EMG wrist-hand motion recognition system for real-time embedded platform," in *Proc. IEEE Int. Conf. Acoust., Speech Signal Process. (ICASSP)*, May 2019, pp. 1523–1527, doi: 10.1109/ICASSP.2019.8683104.
[37] X. Zhou, S. Li, C. Liu, H. Zhu, N. Dong, and T. Xiao, "Non-intrusive load monitoring using a CNN-LSTM-RF model considering label correlation and class-imbalance," *IEEE Access*, vol. 9, pp. 84306–84315, 2021, doi: 10.1109/ACCESS.2021.3087696.
[38] E. V. Fuentes, F. Déniz, and A. V. Martínez, "Electric vehicle grid integration analysis in low voltage networks—A case study," in *Proc. Int. Conf. Mod. Elect. Power Eng. (ICMEPE)*, vol. 1, no. 3, 2016, p. 4.
[39] D. M. Laverty, R. J. Best, P. Brogan, I. Al Khatib, L. Vanfretti, and D. J. Morrow, "The OpenPMU platform for open-source phasor measurements," *IEEE Trans. Instrum. Meas.*, vol. 62, no. 4, pp. 701–709, Apr. 2013, doi: 10.1109/TIM.2013.2240920.
[40] A. F. M. Jaramillo, D. M. Laverty, J. M. del Rincon, J. Hastings, and D. J. Morrow, "Supervised non-intrusive load monitoring algorithm for electric vehicle identification," in *Proc. IEEE Int. Instrum. Meas. Technol. Conf. (IMTC)*, May 2020, pp. 1–6, doi: 10.1109/I2MTC43012.2020.9128529.
[41] A. A. Munshi and Y. A.-R. I. Mohamed, "Unsupervised nonintrusive extraction of electrical vehicle charging load patterns," *IEEE Trans. Ind. Informat.*, vol. 15, no. 1, pp. 266–279, Jan. 2019, doi: 10.1109/TII.2018.2806936.
[42] S. Burns and O. Khan. (Aug. 2013). *LCN Fund Tier 1, Close Down Report: LV Current Sensor Technology Evaluation*. Accessed: Sep. 10, 2022. [Online]. Available: https://www.westernpower.co.uk/projects/lv-sensors
[43] A. F. M. Jaramillo, J. Lopez-Lorente, P. Brogan, D. Laverty, J. M. del Rincon, and A. Foley, "Impact assessment of NILM methods for an enhanced observability of low voltage distribution networks," in *Proc. IEEE Int. Smart Cities Conf. (ISC)*, Sep. 2022, pp. 1–7, doi: 10.1109/ISC255366.2022.9922230.

ANDRES F. MORENO JARAMILLO (Member, IEEE) was born in Medellin, Colombia, in 1990. He received the B.Eng. degree in control engineering from the Universidad Nacional de Colombia, in 2012, the M.Sc. degree in power engineering and sustainable energy from Swansea University, U.K., in 2018, and the Ph.D. degree in electrical and electronic engineering from the Energy, Power, and Intelligent Control (EPIC) Cluster, Queen's University Belfast, U.K., in 2022. He has five years of professional experience in the development of control and automation projects for the chemical, mining, and renewable energy sectors. Subsequently, he joined the Future Networks Team, NIE Networks, Northern Ireland. His research interests include LV monitoring, data analytics, and machine learning, for an increasing hosting capacity of distributed energy resources (DER) in low-voltage distribution networks.

JAVIER LOPEZ-LORENTE (Member, IEEE) received the B.Sc. degree in electrical engineering and the M.Sc. degree in sustainable energy technologies from the Polytechnic University of Valencia, Valencia, Spain, in 2013 and 2015, respectively, and the Ph.D. degree in electrical and electronic engineering from Queen's University Belfast, Belfast, U.K., in 2021. He is currently a Postdoctoral Researcher with the PV Technology Laboratory, FOSS Research Centre for Sustainable Energy, University of Cyprus, Nicosia, Cyprus. His research interests include solar resource assessment, short-term irradiance variability and forecasting, grid impact analysis of variable renewable energy sources, and energy storage systems.

DAVID M. LAVERTY (Senior Member, IEEE) received the M.Eng. and Ph.D. degrees from Queen's University Belfast, U.K., in 2006 and 2010, respectively. He is currently a Reader with the Energy, Power, and Intelligent Control Cluster, Queen's University Belfast. His research interests include anti-islanding detection, telecommunications, cyber-security, and synchrophasor measurement. He is an Associate Editor of the IEEE Open Access Journal of Power and Energy.

PAUL V. BROGAN received the M.Sc. and Ph.D. degrees from Queen's University Belfast, Belfast, U.K., in 2009 and 2016, respectively. His Ph.D. research was in wide-area monitoring, protection and control, and utilizing PMU measurements. His postdoctoral research was in large-scale battery energy storage for network services with a focus on monitoring battery operation and optimization. He is currently working as an Employee, a Founder, and the Director of Phasora Ltd., which is developing a high-precision power system monitoring device.

SANTIAGO H. HOYOS VELASQUEZ (Member, IEEE) received the master's and Ph.D. degrees in engineering applied to energy systems. He is an electrical and systems engineer. In his 20 years of experience in the energy sector, he has worked as a manager, a project director (project management professional), and an energy analyst. He has worked in engineering and consulting companies. He was recently a Technical Coordinator of FENOGE attached to the Ministry of Mines and Energy of Colombia. In addition, he has more than 15 years of experience in the academic sector, as a senior lecturer and a researcher in the areas of renewable energy, energy markets, energization of non-interconnected zones, systems thinking, modeling and simulation, decision analysis, strategy, algorithms, and programming.

JESUS MARTINEZ-DEL-RINCÓN received the B.Sc. degree in telecommunication engineering and the Ph.D. degree in computer vision from the University of Zaragoza, Zaragoza, Spain, in 2003 and 2008, respectively, for his work into the development of tracking algorithms for video surveillance and human motion analysis. He is currently a Senior Lecturer with the School of Electronics, Electrical Engineering and Computer Science, Queen's University Belfast, Belfast, U.K. His main research interests include deep learning applied to video surveillance and cybersecurity.

AOIFE M. FOLEY (Senior Member, IEEE) received the B.E. degree in civil engineering and the Ph.D. degree in unit commitment modelling of wind and energy storage in the Irish power system from the University College Cork, Cork, Ireland, in 1996 and 2011, respectively, and the M.Sc. degree in transportation engineering from Trinity College, Dublin, Ireland, in 1999. She is Chair in Net Zero in the School of Engineering at The University of Manchester, U.K. and Professor in Energy Systems Engineering with the School of Mechanical and Aerospace Engineering, Queen's University Belfast, Belfast, U.K. She worked in industry for 12 years for ESB International, Siemens, SWS Energy and PM Group, in the development, planning, design, and management of energy, telecoms, waste, and pharma projects. Her research interests include energy systems modelling focused on electricity systems, markets and services, wind power, electric vehicles, and smart technologies. Dr. Foley is the Editor in Chief of Renewable and Sustainable Energy Reviews. She was a founding member of the IEEE VTS U.K. and Ireland Chapter in 2011. She is a Chartered Engineer (2001), a Fellow of Engineers Ireland (2012), and a member of the IEEE PES and VTS.